

Bolometric detection of quantum shot noise in coupled mesoscopic systems

Masayuki Hashisaka, Yoshiaki Yamauchi, Shuji Nakamura, Shinya Kasai, Teruo Ono, and Kensuke Kobayashi
Institute for Chemical Research, Kyoto University, Uji, Kyoto 611-0011, Japan

(Received 17 October 2008; revised manuscript received 14 November 2008; published 17 December 2008)

We demonstrate a scheme to detect the quantum shot noise in coupled mesoscopic systems. By applying the noise thermometry to the capacitively coupled quantum point contacts (QPCs) we prove that the noise temperature of one QPC is in perfect proportion to that of the other QPC which is driven to nonequilibrium to generate quantum shot noise. The present mesoscopic bolometry, which is sensitive to the energy flow of ~ 1 fW, allows us to detect the energy exchange between quantum systems at finite frequency and can also be applied for diverse precise measurements.

DOI: [10.1103/PhysRevB.78.241303](https://doi.org/10.1103/PhysRevB.78.241303)

PACS number(s): 73.23.Ad, 72.70.+m, 73.50.Lw, 73.50.Pz

Detection of the quantum-mechanical states in two-level systems (TLSs) is a key technique for quantum information technology.^{1,2} The coupled mesoscopic device of a quantum dot (QD) and a quantum point contact (QPC) is one of the promising candidates of the qubit as an ideal combination of a TLS and a fast read-out scheme.^{2,3} The most significant drawback of this technique is, however, the decoherence of the quantum states in the QD caused by the back action from the QPC due to the shot noise.⁴⁻⁷ The recent study on the nonlocal noise detection by using TLSs (Ref. 8) illustrates the significance of the back action in the QD-QPC coupled systems.⁹⁻¹¹ In the experiments on the QD-QPC system,^{10,11} it is demonstrated that the high-frequency noise is converted to the dc signal by using the energy level separations in the QD, resulting in the very high sensitivity in the narrow bandwidth as a nonlocal noise detection scheme. In order to develop a less disturbing scheme for the quantum state read out, it is necessary to evaluate and minimize the total disturbance due to the shot noise, which has not been performed so far.

In this Rapid Communication, we report the on-chip bolometric noise detection scheme; the shot noise generated in one QPC is detected by using the other QPC in the capacitively coupled double QPC (DQPC) system. The capacitors are designed to electrically decouple the two QPCs at low frequencies and also designed to transfer the high-frequency noise from one to the other. As the QPC constitutes the energy continuum, the electrical fluctuation in the source QPC can be detected for large frequency bandwidth, enabling us to evaluate the total disturbance by using the precise noise thermometry^{12,13} in the detector QPC, which is at the heart of our experiment. We also found an unexpected effect that the source QPC seems to be “cooled” by the detector QPC, which would be potentially useful for the less disturbing charge-detection scheme.

Figure 1(a) shows the scanning electron microscope image of the DQPC device fabricated on the GaAs/AlGaAs two-dimensional electron gas [(2DEG): electron density $= 2.3 \times 10^{11}$ cm⁻² and mobility $= 1.1 \times 10^6$ cm²/V s] and the measurement setup. The DQPC was realized by applying the negative voltages to the side gate electrodes (V_1 and V_2) with applying fixed negative voltages to the center gate electrodes ($V_L = -1.4$ V and $V_R = -1.8$ V). We applied finite dc source-drain voltages (V_{SD}) to QPC1 (source QPC) to produce shot noise while QPC2 (detector QPC) was kept unbiased. The

characteristic of the conductance of QPC2 (G_2) as a function of V_2 is shown in the inset of Fig. 1(c). Throughout our experiment, G_2 was fixed to $2e^2/h \cong (12.9 \text{ k}\Omega)^{-1}$, namely, at the center of the first conductance plateau. The current noises in QPC1 and QPC2 were individually and simultaneously obtained by measuring the voltage fluctuation at the resonant circuits at 3.0 MHz through the two signal amplifying lines.¹⁴⁻¹⁷ The noise measurements were performed by capturing the time domain data and converting the data to spectral density signals by the two-channel digitizer. The experiment was performed in the dilution refrigerator whose base temperature is 45 mK and the electron temperature (T_e) in the equilibrium states was estimated to be 125 mK by measuring the thermal noise of the QPC. We applied a slight magnetic field (0.2 T) perpendicular to the 2DEG as performed in Refs. 15 and 18.

Now we show how the bolometric detection works in this system. Figures 1(b) and 1(c) show the typical results of the noise measurements obtained at different V_{SD} for QPC1 and QPC2, respectively. The conductance of the source QPC1 (G_1) measured simultaneously with the noise measurements is also shown in Fig. 1(b) (the right axis). For $V_{SD} = 0$ μ V, the behavior of the current noise in QPC1 exactly traces that of G_1 as a function of V_1 as expected for the thermal noise at T_e . In general, the shot noise occurs at finite V_{SD} due to the partition process of electrons at the QPC.¹⁸⁻²⁰ In the low-frequency limit, the power spectral density of the current noise (S_I) is given as follows:

$$S_I(V_{SD}) = 4k_B T_e G + 2FG \left[eV_{SD} \coth\left(\frac{eV_{SD}}{2k_B T_e}\right) - 2k_B T_e \right], \quad (1)$$

where G is the conductance of the QPC, F is the Fano factor expressed as $F = \sum_n T_n(1 - T_n) / \sum_n T_n$ (T_n is the transmission of the n th channel in the QPC), k_B is the Boltzmann constant, and $-e$ is the charge of the electron. The measured noise in the source QPC1 (S_I^{QPC1}) shown in Fig. 1(b) qualitatively agrees with the above theory; S_I^{QPC1} peaks as a function of V_1 when G_1 is around half integer of $2e^2/h$, while it is suppressed at the center of the conductance plateaus [quantitative analysis will be discussed later in Fig. 4(b)]. On the other hand, although the detector QPC2 is kept unbiased, the noise in QPC2 (S_I^{QPC2}) increases according to the increase in

S_I^{QPC1} [Figs. 1(c) and 1(d)]. Note that the current noise in the detector S_I^{QPC2} is observed to be only sensitive to the bias-dependent excess noise in the source QPC1: the shot noise and the bias-dependent electron heating^{15,18} in QPC1. The thermal noise of QPC2 (S_I^{QPC2} at $V_{\text{SD}}=0$ μV) remains unaffected when G_1 changes as a function of V_1 [see the black curve in Fig. 1(c)], which clearly indicates that two QPCs are electrically decoupled at 3.0 MHz. In addition, Fig. 1(d) tells us that no finite dc is produced at QPC2 by the dc flowing across QPC1, which excludes the possibility of the Coulomb-mediated or phonon-mediated drag effects.^{21–23} We confirmed that no appreciable cross-correlated signal between QPC1 and QPC2 was detected at 3.0 MHz. The above findings clearly prove that QPC2 exactly works as a nonlocal shot noise detector,²⁴ while two QPCs are electrically decoupled at dc and 3.0 MHz.

We explain the mechanism of this nonlocal shot noise detection as follows: (1) at finite V_{SD} , the high-frequency current fluctuation occurs due to the shot noise in the source QPC1; (2) the high-frequency fluctuation is conducted from QPC1 to the detector QPC2 via the capacitance of the center gate electrodes (C_g); and (3) the transferred fluctuation in QPC2 is energetically relaxed in 2DEG of QPC2 to increase S_I^{QPC2} . In the first process, the spectral density of the high-frequency quantum shot noise for the emission side ($\omega > 0$) in the low-temperature limit ($\hbar\omega \gg k_B T_e$) is represented as⁹

$$S_I^{\text{shot}}(\omega) = \frac{4e^2}{h} \sum_n T_n (1 - T_n) \frac{eV_{\text{SD}} - \hbar\omega}{1 - \exp[-(eV_{\text{SD}} - \hbar\omega)/k_B T_e]}, \quad (2)$$

In the second process, the transport of the noise in the DQPC system is explained by using the electric circuit model shown in Fig. 2(a). QPC1 and QPC2 are capacitively coupled through C_g which was geometrically designed to be about 200 fF. C_g is sufficiently small that QPC1 and QPC2 are electrically disconnected for the low frequency (dc–100 MHz), while C_g can transfer signals above ~ 1 GHz from QPC1 to QPC2. In fact, the voltage fluctuation in the detector QPC2 (S_V^{QPC2}) caused by the current fluctuation at the source QPC1 (Refs. 8–10) is given as $S_V^{\text{QPC2}}(\omega) = |Z(\omega)|^2 S_I^{\text{QPC1}}(\omega)$, where the transimpedance $Z(\omega) = 2iR_1R_2r^2\omega C_g [(R_1+2r)(R_2+2r) + 2i(R_1R_2+R_1r+R_2r)r\omega C_g]^{-1}$. Here R_1 , R_2 , and r are the resistances of QPC1, QPC2, and the four relevant ohmic contacts. The simulated $S_I^{\text{QPC1}}(\omega)$ and $S_V^{\text{QPC2}}(\omega)$ in the equivalent circuit [Fig. 2(a)] with the typical values are presented in Fig. 2(b) with $|Z(\omega)|$ shown in the inset, meaning that the detector, QPC2, can detect the gigahertz fluctuations at the source, QPC1.

As the two QPCs are electrically decoupled at 3.0 MHz, the increase in the thermal noise in the detector QPC2 at this frequency is beyond the circuit model and, therefore, we have to assume the presence of the rapid energy relaxation process of the transmitted gigahertz fluctuations to the lower frequencies. Such downconversion of the high-frequency noise is a direct result of the many-body correlation in 2DEG. As the gigahertz fluctuation dissipates in QPC2 and is absorbed by the thermal bath cooled by the dilution refrig-

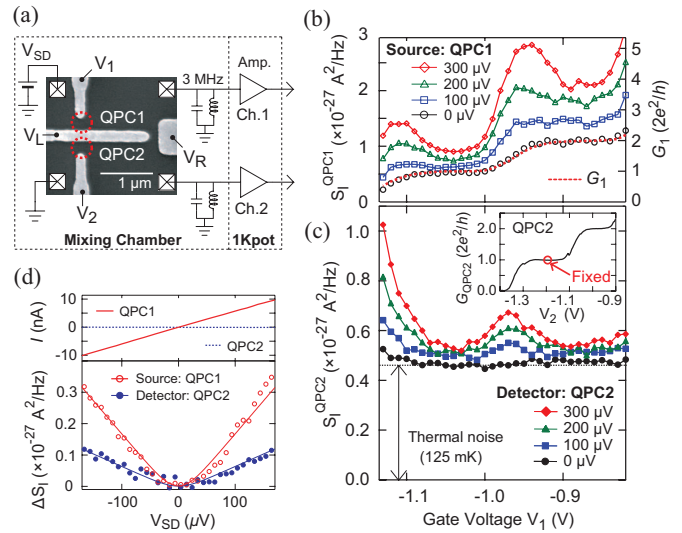


FIG. 1. (Color) (a) Schematic diagram of the measurement setup with the scanning electron microscope image of the sample fabricated on 2DEG. (b) Current noises in QPC1 (S_I^{QPC1}) measured at several source-drain bias voltages ($V_{\text{SD}}=0, 100, 200,$ and 300 μV) are shown (in the left axis) with the conductance of QPC1 (in the right axis) as a function of V_1 . (c) Current noises in QPC2 (S_I^{QPC2}) as a function of the gate voltage V_1 at several V_{SD} for QPC1. The inset shows the conductance of QPC2 as a function of V_2 . (d) dc and excess current noise (ΔS_I ; thermal noise is subtracted) in QPC1 and QPC2 as a function of V_{SD} measured at $V_1=-1.10$ V.

erator, the energy continues to be transferred from QPC1 to QPC2. The energy-exchange process can be regarded as the absorption of energy from a high-temperature nonequilibrium system (QPC1) to a low-temperature system (QPC2).²⁵

To be more quantitative, we compare the excess noise temperature of the detector QPC2 (ΔT_N^{QPC2}) defined by $S_I^{\text{QPC2}} = 4k_B(T_e + \Delta T_N^{\text{QPC2}})G_2$ with the theoretical excess noise temperature of the source QPC1 (ΔT_N^{th}) derived from Eq. (1) in Figs. 3(a) and 3(b). Clearly, ΔT_N^{QPC2} is proportional to ΔT_N^{th} , indicating that the source QPC1 behaves to the detector QPC2 as if it is the heater with the excess temperature of ΔT_N^{th} . Now, we estimate the energy transferred from QPC1 to QPC2 as well as the efficiency of QPC2 detector as a bolometer. In Fig. 4(a) where the measured ΔT_N^{QPC2} at $V_{\text{SD}}=300$ μV is shown in the right axis, we found that ΔT_N^{QPC2} is perfectly proportional to the Fano factor expected for QPC1. We define the efficiency (A) as a scaling factor of F ($F^* = A \times F$), where the rescaled Fano factor F^* is obtained from the fitting for the measured current fluctuation [see Fig. 1(d)] by the following fitting function:

$$S_I^{\text{QPC2}}(V_{\text{SD}}) = 4k_B T_e G_2 + 2F^* G_2 \left[eV_{\text{SD}} \coth\left(\frac{eV_{\text{SD}}}{2k_B T_e}\right) - 2k_B T_e \right]. \quad (3)$$

The obtained efficiency $A=0.15$ [see Fig. 4(a)] implies that at least 15% of the energy generated by the shot noise in the biased QPC1 is continuously absorbed by QPC2.²⁶ This estimation gives the lower limit of the transferred energy

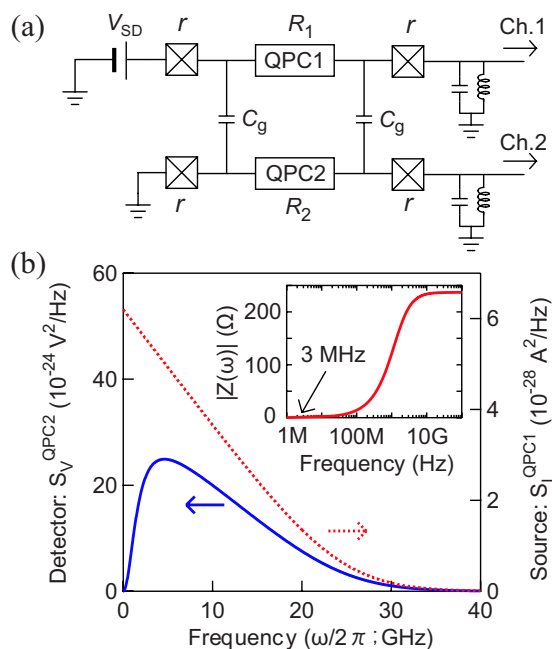


FIG. 2. (Color online) (a) Electrical circuit model of the present setup. The capacitances of the center gates (C_g) between the leads of the QPCs were designed to be $C_g \sim 200$ fF. The typical resistance of the ohmic contacts (r) including the lead resistances were 250Ω . (b) Current fluctuation at the source QPC1 (dotted red/gray line) and the voltage fluctuation at the detector QPC2 (blue/dark gray line) for the finite frequency calculated for $G_1 = e^2/h$ ($F=0.5$), $V_{SD}=100 \mu\text{V}$, $G_2=2e^2/h$, and $T_e=125$ mK. The inset shows the frequency dependence of the absolute value of the transimpedance $Z(\omega)$. The thermal noise is not taken into account in this plot.

which depends on the thermal conductivity in QPC2 since QPC2 is connected to the thermal bath of the dilution refrigerator; if the thermal conductivity is lower, A becomes larger and vice versa. The emission power from the source to the detector is also estimated to be $\int d\omega |Z(\omega)| S_I^{\text{QPC1}}(\omega) \cong 1.7$ fW for the same parameters as in Fig. 2(b), which gives the typical sensitivity of our bolometer.^{27,28}

So far we have focused ourselves in establishing that the quantum noise of QPC1 “heats” QPC2. What happens in our noise source QPC1? In Fig. 4(b), we plot the observed excess noise temperature and the Fano factor in the source

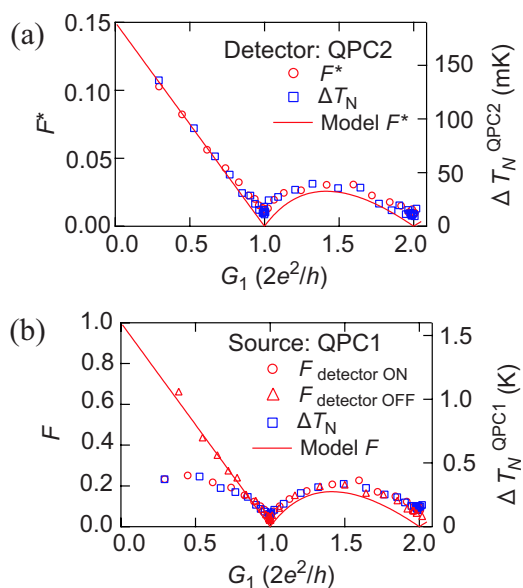


FIG. 4. (Color online) (a) Excess noise temperature at $V_{SD} = 300 \mu\text{V}$ (blue/dark gray square: right axis) and the estimated rescaled Fano factor for QPC2 (red/gray circle: left axis) as a function of the conductance of QPC1. The behavior was well fitted with the rescaled Fano factor (red/gray line) by using Eq. (3). (b) As a function of the conductance of QPC1 are plotted the excess noise temperature at $V_{SD}=300 \mu\text{V}$ (blue/dark gray square: right axis) and the estimated Fano factor (red/gray circle: left axis) for QPC1 with QPC2 fixed at the first conductance plateau, namely, with the detector “switched on.” We also plot the Fano factor for QPC1 (red/gray triangle: left axis) when the resistance of QPC2 is set to $\sim 0 \Omega$, namely with the detector “switched off.”

QPC1 when the detector QPC2 was fixed at the first conductance plateau [see the inset of Fig. 1(c)]. Experimentally, we found that the excess noise temperature of QPC1 defined as above (ΔT_N^{QPC1}) is significantly lower than ΔT_N^{th} at the low conductance region ($G_1 < 2e^2/h$). In contrast, in Fig. 4(b), we superpose the Fano factor obtained when the resistance of QPC2 was set to $\sim 0 \Omega$ ($V_2=0$ V), which gives the Fano factor as the theory expects. Although we do not fully understand the reason for this unexpected observation, one possible explanation would be the inverse process of the “heating” effect by the source: the detector QPC2 “cools” the

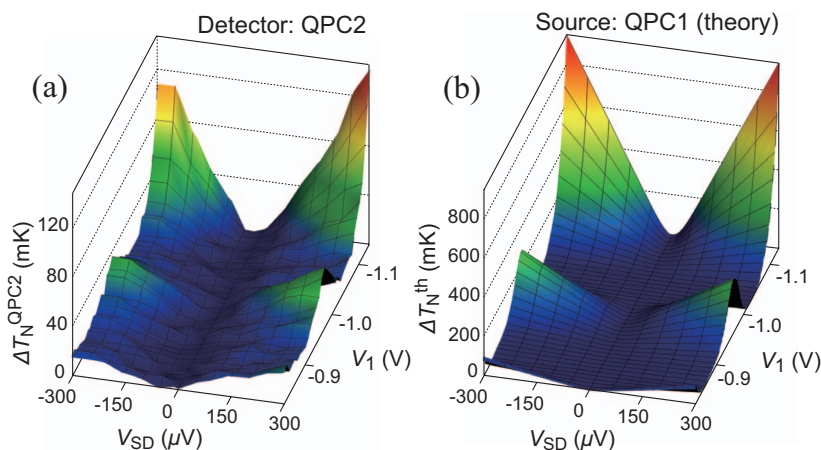


FIG. 3. (Color) (a) Three-dimensional (3D) image plot of the excess noise temperature measured for the detector QPC2 (ΔT_N^{QPC2}). The horizontal axes are the gate voltage V_1 and the source-drain voltage V_{SD} applied to the source QPC1, respectively. (b) Corresponding 3D image plot of the excess noise temperature in the source QPC1 (ΔT_N^{th}) calculated based on the standard shot noise theory.

source QPC1 by absorbing the high-frequency shot noise component presumably because QPC2 works as a dissipative environment for QPC1.²⁹ The suppression of the noise temperature becomes striking with the decrease in G_1 . However, the effect is little, if any, at $G_1 > 2e^2/h$, while the energy absorption by QPC2 occurs as QPC2 detects the correct shot noise [Fig. 4(a)]. Insufficiency of the resolution of our measurement system or other essential energy transfer mechanisms may prevent us to detect the small decrease at the higher conductance region. Note that the partition process at QPC1 is never affected by the presence of the detector QPC2, while the removal of the high-frequency noise results in the reduced fluctuation in QPC1. Further investigation of the “cooling” effect would be useful in creating less disturbing and more accurate charge read-out scheme in the QD-QPC system, where the shot noise would not give the principle limit of accuracy.³⁰

To conclude, we demonstrate the mesoscopic bolometry in the capacitively coupled double QPCs, where the shot noise at one QPC is detected by the increase in the noise

temperature of the other QPC. While the shot noise is described in the scattering theory in quantum mechanics,¹⁹ it can heat materials by being dissipated when the system is connected to the other with the appropriate impedance. We have also found that the inverse process, namely, the cooling effect might be present, which may be useful in creating less disturbing charge read-out scheme in the QD-QPC system. Moreover, the simple detection scheme of the present noise bolometry makes it attractive for diverse ultraprecise measurements such as in the bolometric photon counting and the advanced metrology.

We appreciate fruitful discussions with R. Leturcq, Y. Chung, S. Gustavsson, C. Strunk, P. Roche, T. Martin, Y. Utsumi, T. Fujii, and K. Matsuda. This work was supported by KAKENHI, Yamada Science Foundation, and Matsuo Science Foundation. M.H. is thankful for the financial support by SCAT and JSPS Research Foundation for Young Scientists.

-
- ¹M. A. Nielsen and I. L. Chuang, *Quantum Computation and Quantum Information* (Cambridge University Press, Cambridge, 2000).
- ²D. Awschalom, D. Loss, and N. Samarth, *Semiconductor Spintronics and Quantum Computation* (Springer-Verlag, Berlin, 2002).
- ³R. Hanson *et al.*, *Rev. Mod. Phys.* **79**, 1217 (2007), and references therein.
- ⁴I. L. Aleiner, N. S. Wingreen, and Y. Meir, *Phys. Rev. Lett.* **79**, 3740 (1997).
- ⁵Y. Levinson, *Europhys. Lett.* **39**, 299 (1997).
- ⁶E. Buks, R. Schuster, M. Heiblum, D. Mahalu, and V. Umansky, *Nature (London)* **391**, 871 (1998).
- ⁷M. Avinun-Kalish, M. Heiblum, A. Silva, D. Mahalu, and V. Umansky, *Phys. Rev. Lett.* **92**, 156801 (2004).
- ⁸R. Deblock, E. Onac, E. Gurevich, and L. P. Kouwenhoven, *Science* **301**, 203 (2003), and its supporting online materials.
- ⁹R. Aguado and L. P. Kouwenhoven, *Phys. Rev. Lett.* **84**, 1986 (2000).
- ¹⁰E. Onac, F. Balestro, L. H. Willems van Beveren, U. Hartmann, Y. V. Nazarov, and L. P. Kouwenhoven, *Phys. Rev. Lett.* **96**, 176601 (2006).
- ¹¹S. Gustavsson, M. Studer, R. Leturcq, T. Ihn, K. Ensslin, D. C. Driscoll, and A. C. Gossard, *Phys. Rev. Lett.* **99**, 206804 (2007).
- ¹²L. Spietz, K. W. Lehnert, I. Siddiqi, and R. J. Schoelkopf, *Science* **300**, 1929 (2003).
- ¹³F. Giazotto, T. T. Heikkilä, A. Luukanen, A. M. Savin, and J. P. Pekola, *Rev. Mod. Phys.* **78**, 217 (2006).
- ¹⁴A. M. Robinson and V. I. Talyanskii, *Rev. Sci. Instrum.* **75**, 3169 (2004).
- ¹⁵L. DiCarlo *et al.*, *Rev. Sci. Instrum.* **77**, 073906 (2006); L. DiCarlo, Y. Zhang, D. T. McClure, D. J. Reilly, C. M. Marcus, L. N. Pfeiffer, and K. W. West, *Phys. Rev. Lett.* **97**, 036810 (2006).
- ¹⁶M. Hashisaka *et al.*, *Phys. Status Solidi C* **5**, 182 (2008).
- ¹⁷M. Hashisaka *et al.*, *J. Phys.: Conf. Ser.* **109**, 012013 (2008).
- ¹⁸A. Kumar, L. Saminadayar, D. C. Glatli, Y. Jin, and B. Etienne, *Phys. Rev. Lett.* **76**, 2778 (1996).
- ¹⁹Y. M. Blanter and M. Büttiker, *Phys. Rep.* **336**, 1 (2000).
- ²⁰M. Reznikov, M. Heiblum, H. Shtrikman, and D. Mahalu, *Phys. Rev. Lett.* **75**, 3340 (1995).
- ²¹P. Debray *et al.*, *J. Phys.: Condens. Matter* **13**, 3389 (2001).
- ²²M. Yamamoto *et al.*, *Science* **313**, 204 (2006).
- ²³V. S. Khrapai, S. Ludwig, J. P. Kotthaus, H. P. Tranitz, and W. Wegscheider, *Phys. Rev. Lett.* **99**, 096803 (2007).
- ²⁴While the shot noise gives the dominant contribution, to be more precise, QPC2 is a nonequilibrium noise detector.
- ²⁵This capacitive coupling model is the most feasible explanation for the bolometric detection because of its high efficiency, while other mechanisms [coupling via phonons (Ref. 23), for example] might also play a role in the energy transfer between the QPCs.
- ²⁶As the nonlocal shot noise detection is caused by the capacitive coupling between two QPCs, it is expected that the efficiency (A) of the nonlocal detection does not depend on the geometrical distance between the source QPC and the detector. We have experimentally confirmed it by using several detectors located a few micrometers (1, 3.5, and 5 μm) away from the source QPC.
- ²⁷The value is overestimated as the transimpedance should be lowered from the estimation in the simple circuit model due to the stray capacitance around the DQPC sample (Ref. 8).
- ²⁸We confirmed the bolometric noise detection when the detector QPC is set to out of the first conductance plateau. The efficiency of the detector monotonously decreases with increasing the conductance of the detector. For example, the detection efficiency with the detector set to the second plateau was 8%.
- ²⁹A. Naik *et al.*, *Nature (London)* **443**, 193 (2006).
- ³⁰L. M. Vandersypen *et al.*, *Appl. Phys. Lett.* **85**, 4394 (2004).